Original Article

A Novel Hybrid DC–CC–Based Reactive Power Compensation Scheme to Improve Power Quality of an Electric Grid Considering the Efficiency of Asynchronous Induction Motors

Tien-Dung Nguyen[1], Anh-Tuan Bui[2], Ngoc-Khoat Nguyen[3], Thi-Duyen Bui[4], Ngoc-Quang Dinh[5], Trung-Dung Pham[6]

[1,3,4]*Faculty of Control and Automation, Electric Power University, Hanoi, Vietnam.*
[2]*Faculty of Electrical & Electronics Engineering, Thuyloi University, Hanoi, Vietnam.*
[5]*Director, Innovative Grid Solutions Vietnam JSC, Hanoi, Vietnam.*
[6]*Faculty of Control Engineering, Le Quy Don Technical University, Hanoi, Vietnam.*

[3]*Corresponding Author : khoatnn@epu.edu.vn*

Abstract - Electric motors, especially large-capacity Induction Motors (IMs), are the main load components and consume most electricity output from industrial zones and factories. As a result, optimizing the efficiency and operation of such loads will significantly improve the power quality and reduce power losses on the grid. A crucial control scheme is to propose an effective way to decline Power Loss (PL) against an overtime-changing network voltage. The present paper introduces a new optimal solution to reduce the PL of industrial production lines embedded in many three-phase asynchronous motors. This study evaluates the influence of voltage fluctuations on three-phase AC motors to propose and design a new-generation voltage regulation system. Such a system consists of distributed reactive power compensation (DC) devices located at the load nodes, and they are monitored and regulated by a common Central Controller (CC). This novel hybrid integration can optimize the production lines' operation mode and the power transmission's efficiency. This work also presents a specific series of steps to address an adequate compensation of reactive power for each induction machine, thereby enhancing the quality of voltage and power at the loads, reducing the loss of active power, and extending the lifespan of the equipment. Furthermore, this work implemented and represented several simulations in Matlab/Simulink and experiments on a practical power system to verify the feasibility of the studied hybrid DC-CC approach.

Keywords - Power quality, DC-CC strategy, Reactive power compensation, Induction motor, NEMA curve.

1. Introduction

Electricity is probably considered to be the lifeblood of every country. Power quality is becoming increasingly important as the economy, science, and technology levels grow. The technology change that makes electricity efficient and economical will greatly benefit manufacturers and consumers.

However, in addition to these technological advances, new equipment and technological lines adversely affect power quality. Therefore, comprehensively solving the power quality problem requires the coordination and efforts of all three parties: electrical equipment manufacturers, power supply units and all electricity users. Solving the problem of improving power quality based on voltage adjustment at electrical loads will help users save energy consumption, reduce costs, and improve productivity and efficiency. It is entirely able to increase the durability of the equipment and ensures the health of electricity users [1-17].

Significant loads in factories and industrial zones are usually asynchronous motors, especially induction machines with huge power capacities. It is a fact that these motors are about 60% of the total load of the distributed electric power grid [18]. When the quality of power is not guaranteed, the PL in most parts of the IMs will increase, increasing the temperature of the machines, shortening the service life, and possibly disrupting the production process. In addition, this phenomenon also affects the electric grid, decreasing the system's power factor and increasing the grid's PL [19-24].

This study focuses on presenting and conducting the following issues:

- Consider the overall problem of PL, including calculating the effects of power quality on the performance of electrical equipment (especially 3-phase induction machines). It should be a problem not considered and calculated in the voltage regulation and reactive power compensation process.
- The voltage deviation affects the motors and electrical energy consumption depending on the type, rated power, and load ratings. When the voltage deviation exceeds allowable levels, the motor's efficiency could be declined [37]. When a decrease of 5% of the voltage appears compared with a rated value, an approximated reduction of 1% regarding the motor's efficiency may appear. When the voltage applied to the motor is reduced by about 10% from the rated voltage, the efficiency declines by 3-4% [22].
- Voltage Fluctuation: The phenomenon of voltage change occurring very quickly in a short time (less than one minute) is called voltage fluctuation. The cause of this phenomenon is mainly dependent upon electrical loads with fast-changing working characteristics (i.e., motors, electric welding machines, arc furnaces), the closing and cutting of renewable energy sources, or the instability of the primary energy source. Voltage fluctuations also cause equipment performance to decrease quickly and affect the health and safety of workers [23]. The voltage fluctuations do not compulsorily exceed 2.5% of the rated voltage [22].
- The effect of unbalanced voltage on the armature of three-phase motors reduces the rated power factor and motor efficiency and increases the power consumption [25-28]. When the voltage imbalances are 2%, 3.5%, and 5%, the power losses increase to 8%, 25%, and 50%, respectively, compared with the rated PL of the motors [19], [29-30]. When the voltage asymmetry is more significant than 5%, the PL across the windings is 90% greater than the rated PL [28], [31]. Therefore, according to international standards, the allowable voltage asymmetry should be less than 2%.
- The voltage harmonic effect causes the resistance and reactance in the rotor circuit to be changed. When the harmonic order increases, the coil's inductance will decrease, and, in the meantime, the resistance and reactance of the coil will increase. As a result, the temperature in most parts of the induction machines varies. In the same harmonic order, the temperature increases as the harmonic value rises. Therefore, the power losses in the IMs will also increase, and the motor efficiency will decrease [18], [32-36].

A solution to the above problems can be conducted successfully with a synchronous procedure, including reactive power compensation, harmonic filtering, and voltage regulation. This increases the network's effectiveness meaningfully, reduces power losses, and improves equipment lifespan [36].

Centralized Compensators (CC) should be generally embedded near the step-down transformer. This characteristic causes the amount of active PL on connecting cables to be not decreased. An extensive occurrence of voltage drops will occur, resulting in a significant decrease in the asynchronous motors' efficaciousness.

Therefore, this work proposes a new voltage regulation strategy applying distributed reactive power compensators (DC) integrated with a Central Controller (CC) considering the power losses of the IMs due to voltage changes to enhance the transmission efficiency of the power grid. As a result, the novel compensation method can be defined as a hybrid DC-CC-based compensation strategy. The core idea of this control scheme is based on successfully solving an optimization problem of power losses.

The current paper is organized as follows. Section 2 will introduce the newly hybrid DC-CC-based reactive power compensation algorithm proposed in this study. A procedure to implement this approach will also be provided. Section 3 represents simulation and experiment results to testify to the applicability of the proposed scheme. At last, several conclusions will be deduced in Section 4 of the current paper.

2. Distributed Compensation Integrated with Central Control (DC-CC) Strategy

The primary influence of power quality on the performance of IMs is the voltage quality consisting of low voltage drop or rise, voltage asymmetry, and harmonics. Therefore, to limit the influence of this problem, this work proposes a voltage control solution using distributed compensators with a centralized control unit (DC-CC strategy).

2.1. One-Line Diagram in a Factory

A typical single-line or one-line diagram representing the electrical system in a factory is shown in Figure 1. Here, MBA – T1 and MBA – T2 are the step-up and step-down transformers. Three IMs, ĐC1, ĐC 2 and ĐC3, are considered three significant grid loads.

Remember that each load containing an asynchronous motor is equipped with a compensator as a distributed compensative controller. At the same time, a centralized one is also embedded in the main bus (see Figure 1). Considering adjusting the reactive power and voltage to minimize the PL in the entire network, this strategy uses distributed reactive power compensation devices.
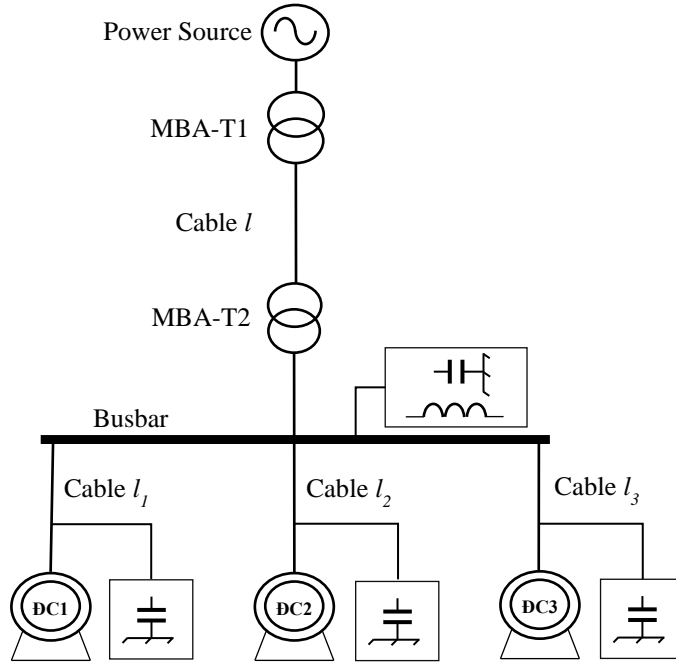
Fig. 1 A typical one-line diagram in a factory with three significant induction loads machines

This system includes compensating devices at each load node, and a control device is placed at the centre. This control part regulates the power flow and supports compensating devices when the voltage drops low or unwanted problems such as voltage asymmetry exist. It is noted that reactive power-compensating elements used to regulate the voltage can be step- or smooth-adjustable devices.

The central device receives all the signals of each load, thereby calculating the compensation capacity for each distributed compensator based on the optimization problem of the PL for the entire plant. In a central control system, it is possible to place additional reactive power compensating devices to supplement or reserve the amount of reactive power that may be lacking for distributed compensation devices.

To calculate optimally PL and compensation capacity for equipment locations in an electric power grid, it should be mandatory to consider the replacement scheme of the network when applying compensating devices, as shown in Figure 2.

2.2. Operation Principle of the System

The central controller calculates the amount of power to be compensated for at each load branch. Subsequently, peripheral devices will be regulated regarding their power and the firing angles' regulation for the compensators located at the centre. When closing a branch of the distributed devices, it is mandatory to combine with the regulation of triggering angle α to be a minimum value $α_{min}$.

This opening angle α will be adjusted until the power is minimized. Peripheral devices' power can be regulated depending on several key factors. They consist of voltage, reactive power, and power factor. A centrally controlled distributed voltage regulator optimizes the lines, compensators, and IM losses. When compensated devices are embedded in the transmission lines, it is necessary to compute several system factors regarding the low-voltage side of the transformer MBA-T2. At this time, the loss of active power caused by the asynchronous motor on the grid when there is a compensating device that ignores the mechanical loss, the loss of the electromagnetic field, etc. [37]:

$$\Delta P = R_{td} \frac{P_{tt}^2 + (Q_{tt} - Q_b)^2}{U_{ht}^2}.10^{-3} + \Delta p_b.Q_b + P_{tt}.\left[-\Delta\eta\{Q_{tt} - Q_b\}\right] \quad (1)$$

Where, R_{td}: resistance value of the power cable connected to the motor i^{th} to the busbar; P_{tt}, Q_{tt}: computed active and reactive power; Δp_b: the active PL of the compensator; Q_b: compensation of reactive power; $\Delta\eta\{Q_{tt} - Q_b\}$ is the efficiency function of the 3-phase IM belonging to reactive power.

The active power losses are divided into three parts as follows:

- The first one is due to residual power flowing into the system and causing losses across the system resistors;
- The second part is the loss in compensating devices;
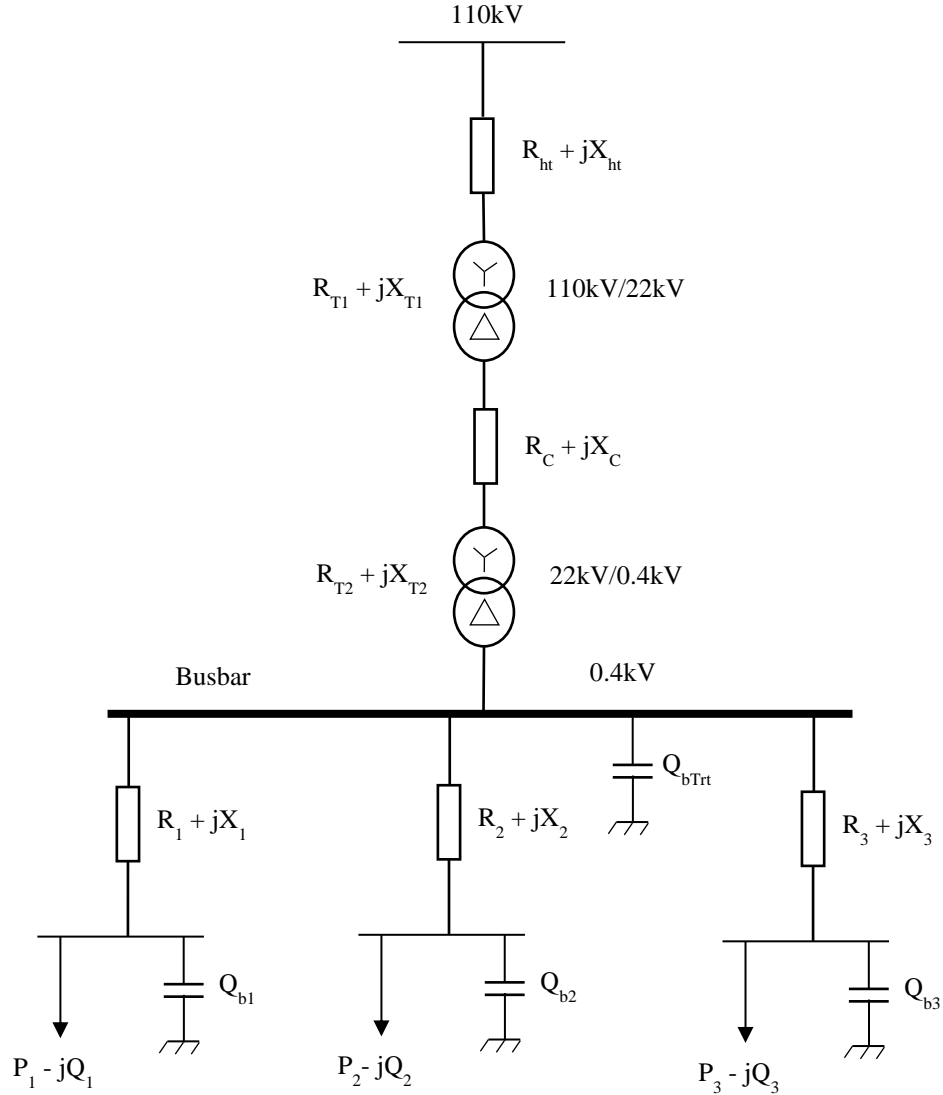- The third unit is the loss in the asynchronous motors;

110kV

Fig. 2 An equivalent diagram for the distributed electric power grid with compensators

To determine the optimal compensating reactive powers, Q_{bi}, the first derivative of the total active PL, should be taken to reach the value of zero. Next, apply the NEMA curve [38], [39] to find the coefficients based on the change in motor efficiency with the variation of voltage:

$$\Delta \eta_i \{Q_i - Q_{bi}\} = (K_1.\Delta U_{DC\_i}^2 + K_2.\Delta U_{DC\_i} + C).10^{-2} \quad (2)$$

Where,
- K_1, K_2 and C are three factors determined based on the experiment curves [38],[39]. These coefficients are ultimately determined for each different type of IMs.
- ΔU_{DC_i} in percent is computed drop motor i^{th} as:

$$\Delta U_{DC\_i} = \frac{U_{TC}.10^3 - U_{dm\_DC} - \Delta U_i}{U_{dm\_DC}}.100 \quad (3)$$

- U_{TC}: busbar voltage (kV);
- U_{dm_DC} rated voltage of the motor (V)
- ΔU_i voltage drop the busbar and motor i^{th}(i:1 ÷ 3) (V):

$$\Delta U_i = \frac{P_i.R_i + (Q_i - Q_{bi})X_i}{U_{TC}} \quad (4)$$

Consider a case study in which a factory consisting of three huge–power IMs is located in different locations. The flowchart representing the proposed optimization algorithm is illustrated in Figure 3. As shown in Figure 3, the procedure of the DC-CC strategy is implemented through the following five steps:

Step 1 : Initialization
In this step, several necessary parameters as an initialization need to be provided.

Step 2 : Approximation of the NEMA curve

Assuming that the NEMA curve is approximated by a parabola in which three factors can be determined: K_1, K_2 and C, as mentioned in (2). These values are found in the Appendix of this paper.

Step 3 : Calculation of the voltage drops ΔU_i and power losses ΔP_i

For an electric power grid loaded with three motors, the total PL is:

$$\Delta P_\Sigma = \sum \Delta P_i + \Delta P_{Trt} \tag{5}$$

Where,

$$\Delta P_i = \Delta P_{cable-i} + \Delta P_{TBb-i} + \Delta P_{IM-i}$$
$$= R_i \frac{P_i^2 + (Q_i - Q_{bi})^2}{U_{TC}^2}.10^{-3} + \Delta p_{bi}.Q_{bi} + P_i \cdot \left[-\Delta \eta_i \{ Q_i - Q_{bi} \} \right] \tag{6}$$

$$\Delta P_{Trt} = R_{td} \frac{P_\Sigma^2 + (Q_\Sigma - Q_{b\Sigma} - Q_{bTrt})^2}{U_{ht1}^2}.10^{-3} + \Delta p_{bTrt}.Q_{bTrt} \tag{7}$$

Step 4 : Solve the optimization constraints

To determine the optimal power losses, this study proposes a new method to solve the following conditions:

$$\begin{cases} \dfrac{\partial \Delta P_\Sigma}{\partial \Delta Q_b} = 0 \\ \dfrac{\partial^2 \Delta P_\Sigma}{\partial Q_b \partial Q_b} = \left[\dfrac{\partial^2 \Delta P_\Sigma}{\partial Q_{bi} \partial Q_{bk}} \right] > 0 \end{cases} \tag{8}$$

Where, two indexes $i, k = \overline{1, 2, 3, Trt}$.

Step 5 : Determination of the optimal power losses and compensated reactive power

After solving the constraint given in (8), the optimal quantities of power losses and reactive power compensation can be obtained. In this stage, the proposed approach is successfully implemented.

3. Numerical Simulation Results and Experiments

3.1. Numerical Simulations

Executing the simulation process is a mandatory phase to verify a new control scheme theoretically. In this section, MATLAB software has implemented several numerical simulations. Here, the five-step procedure indicated in Figure 3 is employed. Simulation parameters and three coefficients of the NEMA curve approximation are provided in the Appendix of this paper.
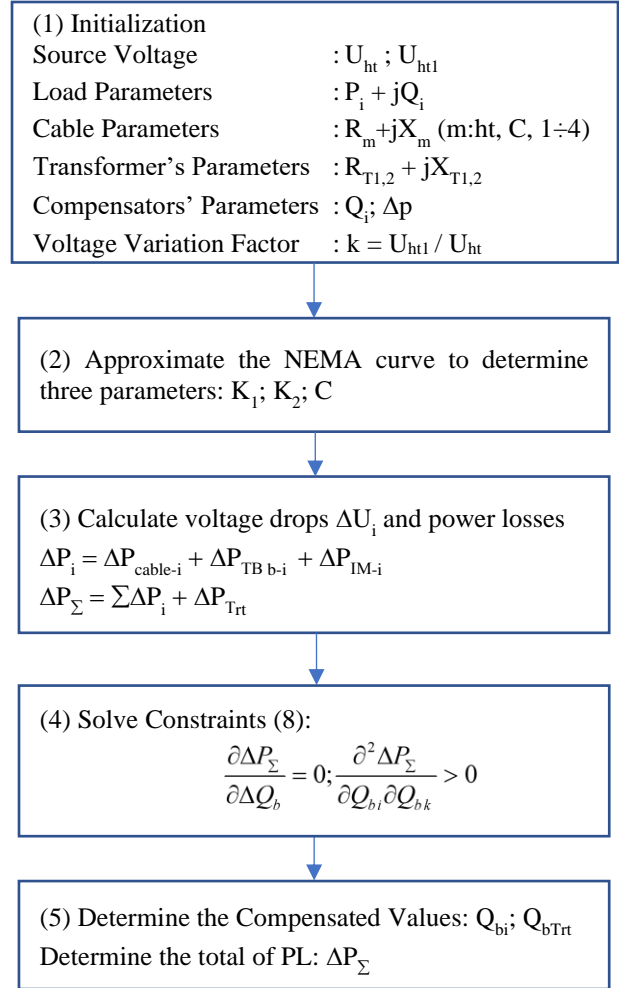
(1) Initialization	
Source Voltage	: U_{ht} ; U_{ht1}
Load Parameters	: $P_i + jQ_i$
Cable Parameters	: $R_m + jX_m$ (m:ht, C, 1÷4)
Transformer's Parameters	: $R_{T1,2} + jX_{T1,2}$
Compensators' Parameters	: Q_i; Δp
Voltage Variation Factor	: $k = U_{ht1} / U_{ht}$

(2) Approximate the NEMA curve to determine three parameters: K_1; K_2; C

(3) Calculate voltage drops ΔU_i and power losses
$\Delta P_i = \Delta P_{cable-i} + \Delta P_{TB\,b-i} + \Delta P_{IM-i}$
$\Delta P_\Sigma = \sum \Delta P_i + \Delta P_{Trt}$

(4) Solve Constraints (8):
$$\frac{\partial \Delta P_\Sigma}{\partial \Delta Q_b} = 0; \frac{\partial^2 \Delta P_\Sigma}{\partial Q_{bi} \partial Q_{bk}} > 0$$

(5) Determine the Compensated Values: Q_{bi}; Q_{bTrt}
Determine the total of PL: ΔP_Σ

Fig. 3 A procedure to perform the simulation process using the MATLAB package

The following two simulation scenarios have been considered to comprehensively evaluate the feasibility of the proposed DC-CC-based reactive power compensation scheme.

3.1.1. Scenario 1

The actual voltages supplied to the motors are supposed to vary in an acceptable range of 90% to 110% from the rated value. A factor k characterizes such a variation; however, it is only assumed to change at instantly different values (five levels: 0.9, 0.95, 1.0, 1.02, 1.05 and 1.1). Simulation results are plotted in Table 1 to Table 3 and Figure 4 to Figure 9. It should be noted that ΔP_4 is denoted for the total losses of cables and transformers.

3.1.2. Scenario 2

The actual voltages have been randomly varied, corresponding to a random factor k from 0.9 to 1.1 (see Figure 10). Simulation results in this perspective are illustrated in Figure 11 and Figure 12.

It is noted that in the First Simulation Scenario (FSC), there are three more minor cases:

Case 1 : No compensation.
Case 2 : Only Distributed Compensators (DC).
Case 3 : Integration of Distributed Compensators and a Central Controller (DC-CC).

From the simulation results, it is meaningful to deduce the following observations:

• When the voltage supplied to the motor increases, the reactive powers required to compensate Q_{bi} for the IMs will decrease. At the same time, the active power losses of the motors ΔP_i and the total loss ΔP_Σ are also reduced.

• The proposed DC–CC–based reactive power compensation method has improved efficiency. The active PL was significantly reduced compared to the uncompensated and distributed compensation (see Figure 5). Meanwhile, the more significant the motor capacities are used, the greater the reduction in active power losses can be obtained. In the simulation case study, with motor 3 (maximum capacity 200kW), the active PL can be reduced by up to 9.5% compared to the only distributed compensation.

• If the voltage is assumed to vary continuously within an allowable amplitude in the Second Simulation Scenario (SSS), the compensating trend of the system and the efficiency of the proposed control solution have remained unchanged. The reactive power to be compensated and the active PL are also variable but within specific allowable ranges, as illustrated in Figure 11 and Figure 12. The voltage regulation, and as a result, the electric power quality, has also been significantly improved when applying the proposed hybrid DC-CC method.

Table 1. Computational results for the FSS: different voltage variation factors

Parameters	U = 0.9Udm			U = 0.95Udm			U = 1.0Udm		
	Case 1	Case 2	Case 3	Case 1	Case 2	Case 3	Case 1	Case 2	Case 3
Qb1 (kVAr)		76.3	105.4		76.3	103.3		76.3	101.0
Qb2 (kVAr)		110.2	135.9		110.2	133.3		110.2	130.5
Qb3 (kVAr)		97.5	123.9		97.5	121.5		97.5	118.9
Power Losses									
ΔP1 (kW)	27.1	21.2	19.3	19.9	15.4	13.8	14.8	11.5	10.0
ΔP2 (kW)	66.6	50.4	47.6	52.1	38.9	36.4	40.9	30.2	27.9
ΔP3 (kW)	46.1	35.3	32.9	35.3	26.6	24.5	27.1	20.3	18.5
ΔP4 (kW)	6.9	5.1	5.0	6.3	4.6	4.5	5.6	4.1	4.1
ΔP$_\Sigma$ (kW)	**146.7**	**112.0**	**104.8**	**113.6**	**85.5**	**79.2**	**88.4**	**66.1**	**60.5**

Table 2. Computational results for the FSS: different voltage variation factors (continued)

Parameters	U = 1.02Udm			U = 1.05Udm			U = 1.1Udm		
	Case 1	Case 2	Case 3	Case 1	Case 2	Case 3	Case 1	Case 2	Case 3
Qb1 (kVAr)		76.3	100.0		76.3	98.4		76.3	95.5
Qb2 (kVAr)		110.2	129.3		110.2	127.4		110.2	124.0
Qb3 (kVAr)		97.5	117.8		97.5	116.0		97.5	112.8
Power losses									
ΔP1 (kW)	13.3	10.3	9.0	11.6	9.2	7.9	10.1	8.6	7.4
ΔP2 (kW)	37.2	27.4	25.3	32.5	24.0	22.1	26.9	20.3	18.5
ΔP3 (kW)	24.5	18.4	16.6	21.4	16.2	14.5	18.0	14.2	12.7
ΔP4 (kW)	5.4	4.0	3.9	5.1	3.7	3.7	4.6	3.4	3.4
ΔP$_\Sigma$ (kW)	**80.4**	**60.1**	**54.8**	**70.6**	**53.1**	**48.2**	**59.6**	**46.5**	**42.0**

Table 3. PL deviations for three cases in the FSS

Voltage Changes	0.9U$_{dm}$	0.95U$_{dm}$	1.0U$_{dm}$	1.02U$_{dm}$	1.05U$_{dm}$	1.1U$_{dm}$
ΔP_Σ (kW) – no compensation (a)	146.7	113.6	88.4	80.4	70.6	59.6
ΔP_Σ (kW) – without a central controller (b)	112.0	85.5	66.1	60.1	53.1	46.5
ΔP_Σ (kW) – with a central controller (c)	104.8	79.2	60.5	54.8	48.2	42.0
Deviations (%): (a) and (b)	23.69%	24.72%	**25.32%**	25.27%	24.73%	22.05%
Deviations (%): (b) and (c)	6.37%	7.35%	8.44%	8.85%	9.35%	**9.58%**
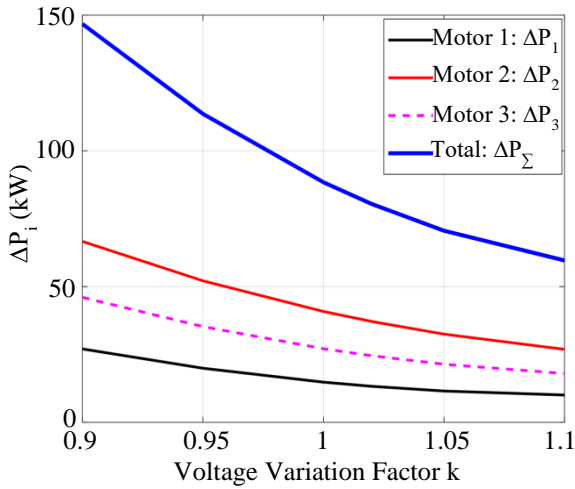
Fig. 4 Power losses in case 1 (uncompensated) – FSS
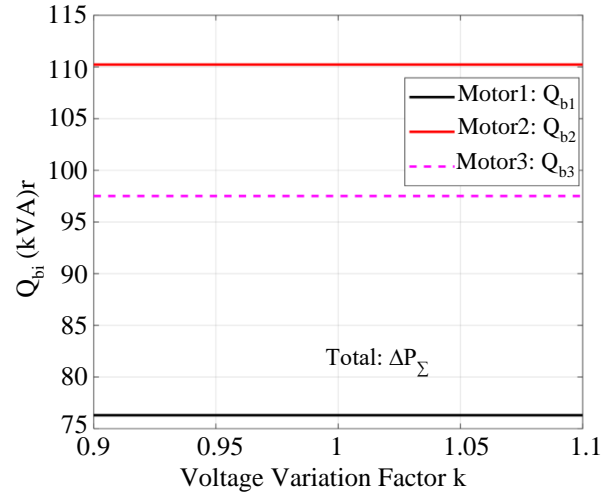
Fig. 6 Reactive power compensations (Q$_{b1}$, Q$_{b2}$, Q$_{b3}$) in case 2 – FSS
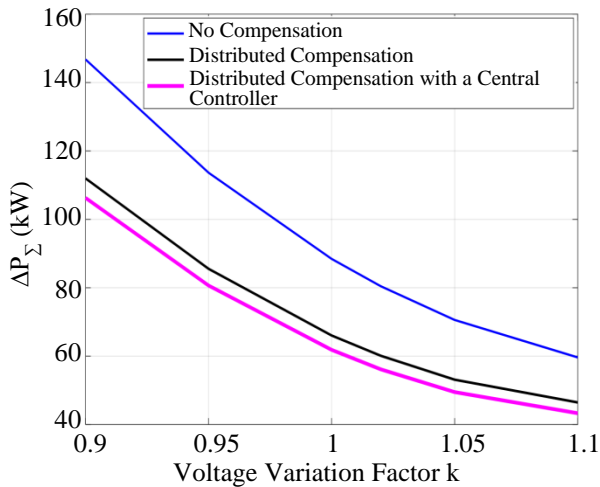
Fig. 5 Comparison of total power losses between three cases – FSS
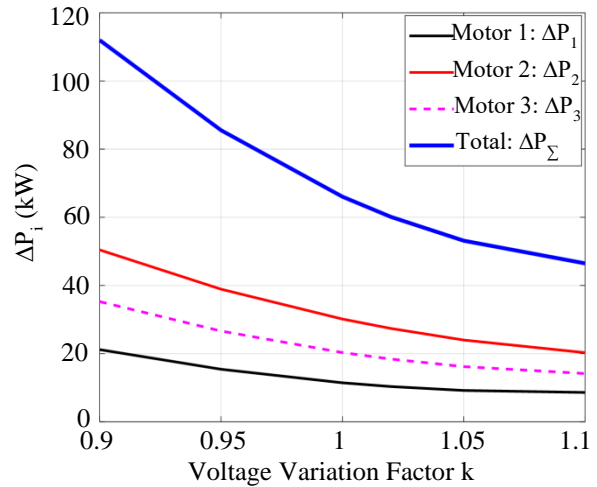
Fig. 7 Power losses for each motor (ΔP_1, ΔP_2, ΔP_3) and their total ΔP_Σ in case 2 – FSS
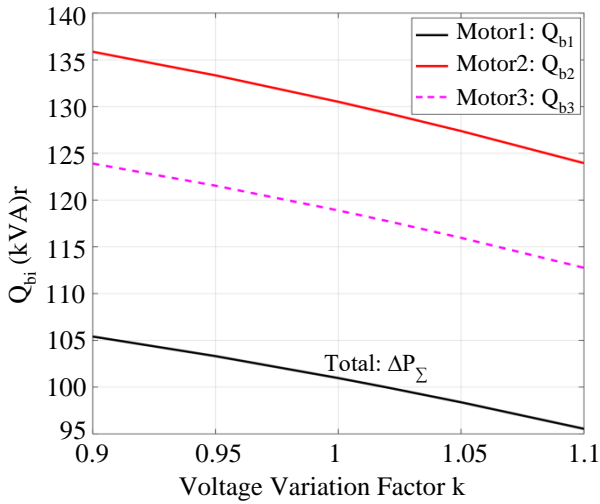
Fig. 8 Reactive power compensations (Q_{b1}, Q_{b2}, Q_{b3}) in case 3 – FSS
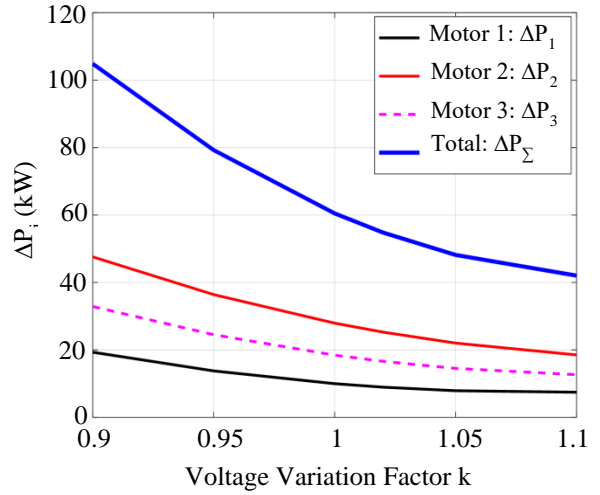
Fig. 9 Power losses for each motor (ΔP_1, ΔP_2, ΔP_3) and their total ΔP_Σ in case 3 – FSS
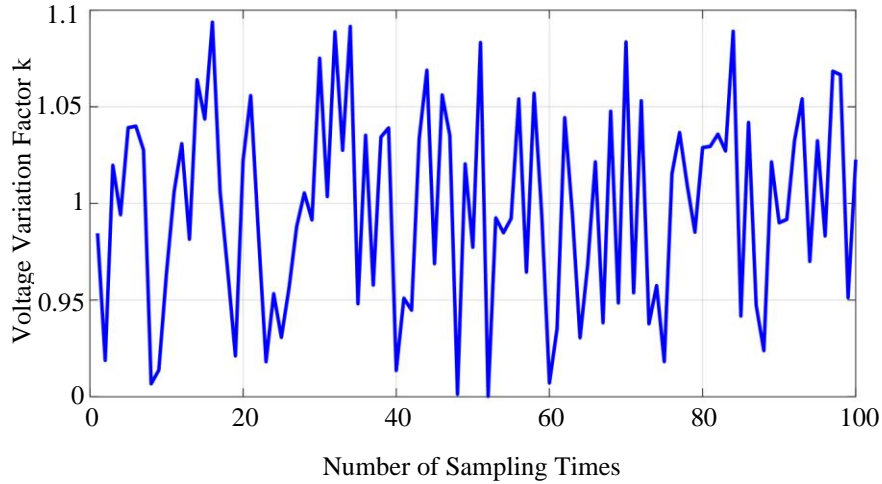

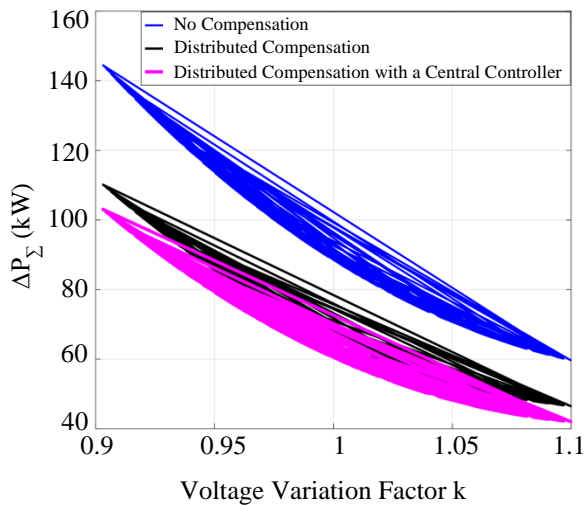**Fig. 10 A random illustration of the voltage variation factor $k = U_{ht1} / U_{ht}$ applied in the SSS**

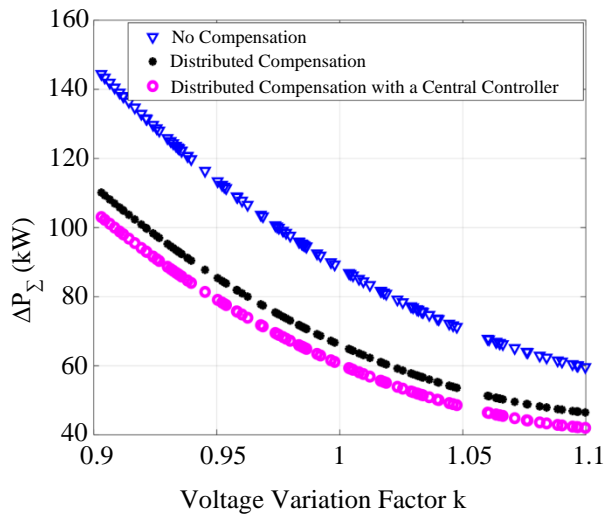**Fig. 11 Comparative results for the second scenario – line curves – SSS**

Fig. 12 Comparative results for the second scenario – point curves - SSS

3.2. Experiment Results

The PL optimization algorithm to improve the power quality proposed in this study has been practically applied to a ministerial-level project in Vietnam, which was successfully defended. A block diagram of the practical control system is shown in Figure 13. It consists of nine modules with different working functions, in which the most important and decisive part is a central controller.

The instrument's control unit includes a measurement circuit used to measure and calculate P, Q, S, frequency, amplitude of harmonics, and the cosφ factor. The central controller handles the parameters and calculations. A Liquid Crystal Display was used to display and monitor the device's parameters. Keyboard device for changing display and setting parameters. The memory helps record the device's

working process in standard modes and analyze the problem. The lights indicate the working status and warnings of the device. The thyristor controller generates pulses to control the switch at the request of the central processor. Finally, DC devices receive control commands from the central controller to locally control capacitors in decentralized compensation.

Several practical main modules, especially the central controller, are successfully designed, manufactured, and testing-installed, as shown in Figure 14 to Figure 19. Experiment results in two contexts, i.e., with the proposed hybrid DC – CC compensation control and without it, have been obtained as given in Table 4. The proposed compensation control strategy achieved much better control criteria, including power losses (active and reactive ones) and power factor cosφ (see Table 4).
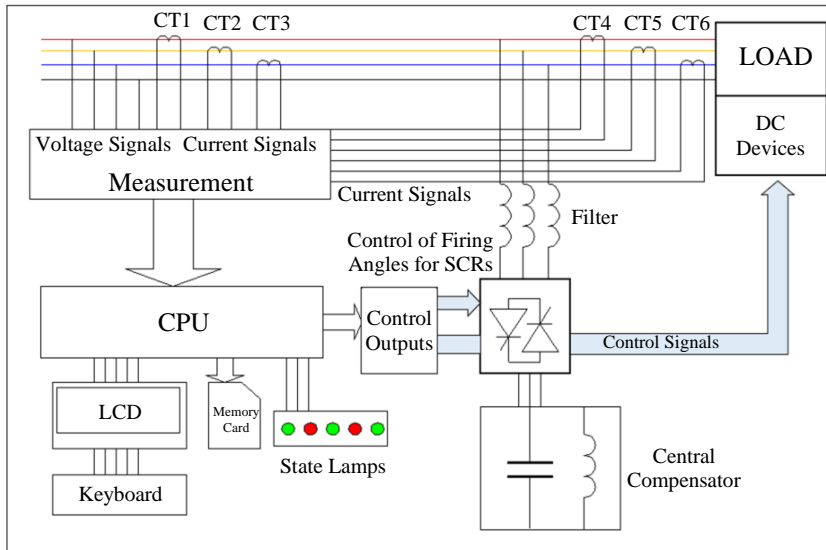

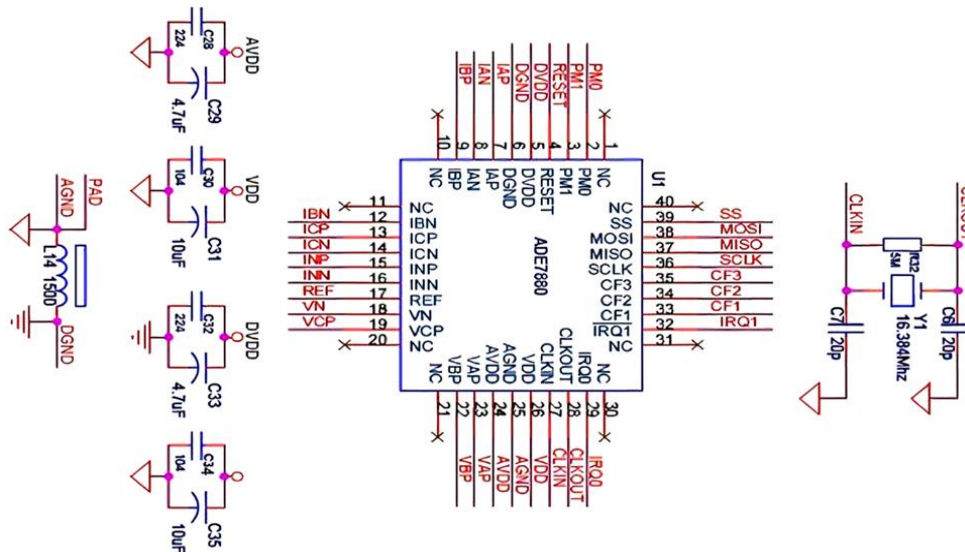**Fig. 13 A block diagram of the proposed hybrid DC-CC compensation strategy applied for experiments**

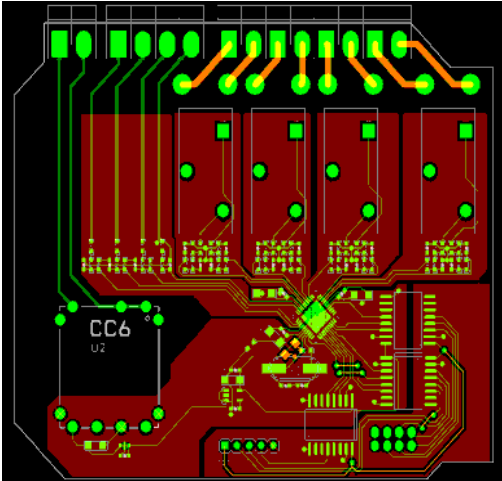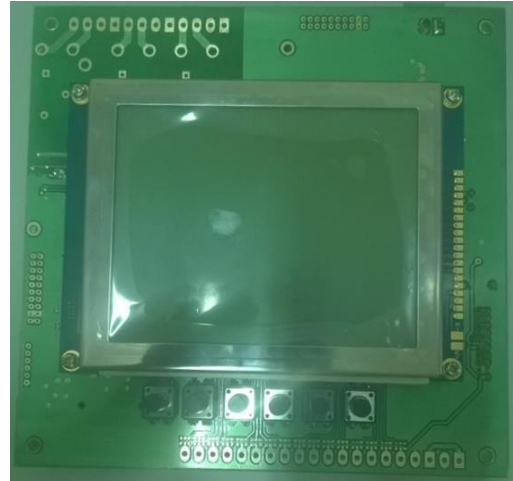**Fig. 14 ADE 7880 used for designing the measurement module**

Fig. 15 The printed circuit board of the measurement module

(a)

Fig. 16 Measurement module of the controller

(b)
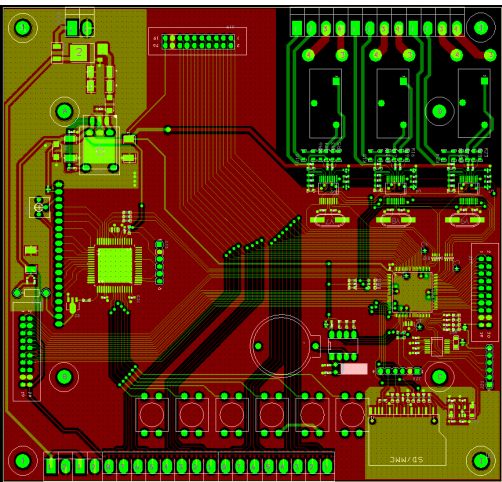**Fig. 18 LCD and practical central control module**

Fig. 17 Printed circuit of the central controller

Fig. 19 The central controller embedded in the electrical control cabinet

Table 4. Comparison between the hybrid DC-CC method and the uncompensated aspect

Operation Modes	Phase	U (V)	I (A)	P_Σ (kW)	Q_Σ (kVAr)	Cosφ
1. The 1st Load (129,1kW; 51KVAr) - (120kW; 28KVAr)						
No Compensation (a)	A	390.8	193.3	129.1	51.5	0.9197
	B	391.5	205.9			
	C	393.5	215.7			
With Compensation (b)	A	392.3	178.7	120.6	28.6	0.9731
	B	393.8	184.4			
	C	395.6	182.4			
Reduction: (a) – (b)		4.8	37.0	8.5	22.9	0.053
2. The 2nd Load (131kW; 55KVAr) - (127kW; -31KVAr)						
No Compensation (a)	A	391.1	219.2	131.0	55.4	0.9509
	B	394.0	191.8			
	C	394.9	219.4			
With Compensation (b)	A	396.1	202.6	127.6	- 31.8	0.9596
	B	399.5	168.0			
	C	400.7	201.1			
Reduction: (a) – (b)		9.6	51.2	3.4	87.2	0.0087
3. The 3rd Load (154kW; 76kVAr) - (145kW; -3,2kVAr)						
No Compensation (a)	A	384.5	245.2	154.0	76.6	0.8687
	B	385.8	282.1			
	C	388.9	245.7			
With Compensation (b)	A	390.4	196.5	145.0	- 3.2	0.9984
	B	391.8	230.0			
	C	394.5	215.8			
Reduction: (a) – (b)		10.0	85.6	9.0	79.8	0.1297

4. Conclusion

A novel DC–CC–based reactive power strategy applied for an electric power grid with significant loads has been proposed in this paper. The main idea of the control procedure depends on the NEMA curve approximation, which is especially suitable for loads of the three-phase IMs and solving the optimization problem of the power losses to find the best capacity of the reactive power compensations.

With five reasonable steps, the algorithm proposed in this study has been entirely able to be implemented in both theoretical and practical domains. Numerical simulation and experiment results shown in this work demonstrated the effectiveness and applicability of the proposed approach. Therefore, the DC-CC strategy significantly contributed to the power network's operation and distribution in Vietnam and other countries.

References

[1] Ching-Tzong Su, and Chih-Cheng Tsai, "A New Fuzzy-Reasoning Approach to Optimum Capacitor Allocation for Primary Distribution Systems," *Proceedings of the IEEE International Conference on Industrial Technology (ICIT'96)*, Shanghai, China, pp. 237-241, 1996. [CrossRef] [Google Scholar] [Publisher Link]

[2] Alireza Askarzadeh, "Capacitor Placement in Distribution Systems for Power Loss Reduction and Voltage Improvement: A New Methodology," *IET Generation, Transmission & Distribution*, vol. 10, no. 14, pp. 3631-3638, 2016. [CrossRef] [Google Scholar] [Publisher Link]

[3] J. Dixon et al., "Reactive Power Compensation Technologies: State-of-the-Art Review," *Proceedings of the IEEE*, vol. 93, no. 12, pp. 2144-2164, 2005. [CrossRef] [Google Scholar] [Publisher Link]

[4] Xuesong Zhou et al., "A Review of Reactive Power Compensation Devices," *2018 IEEE International Conference on Mechatronics and Automation (ICMA)*, Changchun, pp. 2020-2024, 2018. [CrossRef] [Google Scholar] [Publisher Link]

[5] Famous O. Igbinovia et al., "Comparative Review of Reactive Power Compensation Technologies," *2015 16th International Scientific Conference on Electric Power Engineering (EPE)*, Kouty Nad Desnou, Czech Republic, pp. 2-7, 2015. [CrossRef] [Google Scholar] [Publisher Link]

[6] Wolfgang Hofmann, Jürgen Schlabbach, and Wolfgang Just, *Reactive Power Compensation: A Practical Guide*, John Wiley & Sons, Ltd, 2012. [CrossRef] [Google Scholar] [Publisher Link]

[7] H. N. Ng, M. M. A. Salama, and A. Y. Chikhani, "Classification of Capacitor Allocation Techniques," *IEEE Transactions on Power Delivery*, vol. 15, no. 1, pp. 387-392, 2000. [CrossRef] [Google Scholar] [Publisher Link]

[8] S. Jazebi, S. H. Hosseinian, and B. Vahidi, "DSTATCOM Allocation in Distribution Networks Considering Reconfiguration using Differential Evolution Algorithm," *Energy Conversion and Management*, vol. 52, no. 7, pp. 2777-2783, 2011. [CrossRef] [Google Scholar] [Publisher Link]

[9] Vinay M. Awasth, and V. A. Huchche, "Reactive Power Compensation using D-STATCOM," *2016 International Conference on Energy Efficient Technologies for Sustainability (ICEETS)*, Nagercoil, India, pp. 583-585, 2016. [CrossRef] [Google Scholar] [Publisher Link]

[10] Tong XiangQian et al., "Reactive Power and Unbalance Compensation with DSTATCOM," *2005 International Conference on Electrical Machines and Systems*, Nanjing, China, vol. 2, pp. 1181-1184, 2005. [CrossRef] [Google Scholar] [Publisher Link]

[11] Aishvarya Narain, and S. K. Srivastava, "An Overview of Facts Devices Used for Reactive Power Compensation Techniques," *International Journal of Engineering Research & Technology*, vol. 4, no. 12, pp. 81-85, 2015. [CrossRef] [Google Scholar] [Publisher Link]

[12] Vinay N. Sewdien, "Operation of FACTS Controllers," *Flexible AC Transmission Systems*, pp. 1063-1070, 2020. [CrossRef] [Publisher Link]

[13] Imran Khan et al., "Optimal Placement of FACTS Controller Scheme for Enhancement of Power System Security in Indian Scenario," *Journal of Electrical Systems and Information Technology*, vol. 2, no. 2, pp. 161-171, 2015. [CrossRef] [Google Scholar] [Publisher Link]

[14] Madhvi Gupta et al., "Mitigating Congestion in a Power System and Role of FACTS Devices," *Advances in Electrical Engineering*, vol. 2017, pp. 1-7, 2017. [CrossRef] [Google Scholar] [Publisher Link]

[15] Fedor Nepsha et al., "Application of FACTS Devices in Power Supply Systems of Coal Mines," *E3S Web of Conferences*, vol. 174, p. 03026, 2020. [CrossRef] [Google Scholar] [Publisher Link]

[16] Sohrab Mirsaeidi et al., "Optimization of FACTS Devices: Classification, Recent Trends, and Future Outlook," *2021 IEEE 4th International Electrical and Energy Conference (CIEEC)*, Wuhan, China, pp. 1-8, 2021. [CrossRef] [Google Scholar] [Publisher Link]

[17] Abubakar Siddique et al., "A Comprehensive Study on FACTS Devices to Improve the Stability and Power Flow Capability in Power System," *2019 IEEE Asia Power and Energy Engineering Conference (APEEC)*, Chengdu, China, pp. 199-205, 2019. [CrossRef] [Google Scholar] [Publisher Link]

[18] Colin Debruyne, Lieven Vandevelde, and Jan Desmet, "Harmonic Effects on Induction and Line Start Permanent Magnet Machines," *Proceedings of Energy Efficiency of Motor Driven Systems*, pp. 1-10, 2013. [Google Scholar] [Publisher Link]

[19] A. H. Bonnett, "An Overview of How AC Induction Motor Performance has been Affected by the October 24, 1997 Implementation of the Energy Policy Act of 1992," *Record of Conference Papers, IEEE Industry Applications Society 45th Annual Petroleum and Chemical Industry Conference (Cat. No.98CH36234)*, Indianapolis, IN, USA, pp. 149-164, 1998. [CrossRef] [Google Scholar] [Publisher Link]

[20] NEMA, NEMA Standards Publication MG 1-2006 Revision 1-2007, Motors and Generators, National Electrical Manufacturers Association, 2006. [Online]. Available: https://www.nema.org/docs/default-source/standards-document-library/mg-1-2006-rev-1-combined-revised-ed.pdf

[21] A. H. Bonnett, "The Impact that Voltage and Frequency Variations have on AC Induction Motor Performance and Life in Accordance with NEMA MG-1 Standards," *Conference Record of 1999 Annual Pulp and Paper Industry Technical Conference (Cat. No.99CH36338)*, Seattle, WA, USA, pp. 16-26, 1999. [CrossRef] [Google Scholar] [Publisher Links]

[22] Rui Araújo, *Induction Motors - Modelling and Control*, InTech, 2012. [CrossRef] [Google Scholar] [Publisher Link]

[23] Miloje M. Kostic, and Branka Kostic, "Motor Voltage High Harmonics Influence to Efficient Energy Usage," *15th WSEAS International Conference on Systems*, Corfu Island, Greece, pp. 276-281, 2011. [Google Scholar]

[24] Austin H. Bonnett, and Rob Boteler, "The Impact that Voltage Variations have on AC Induction Motor Performance," *American Council for an Energy Efficient Economy*, pp. 301-316, 1999. [Google Scholar] [Publisher Link]

[25] A. Jalilian, and R. Roshanfekr, "Analysis of Three-phase Induction Motor Performance under Different Voltage Unbalance Conditions using Simulation and Experimental Results," *Electric Power Components and Systems*, vol. 37, no. 3, pp. 300-319, 2009. [CrossRef] [Google Scholar] [Publisher Link]

[26] Enrique C. Quispe et al., "Unbalanced Voltages Impacts on the Energy Performance of Induction Motors," *International Journal of Electrical and Computer Engineering (IJECE)*, vol. 8, no. 3, pp. 1412-1422, 2018. [CrossRef] [Google Scholar] [Publisher Link]

[27] J. E. Williams, "Operation of 3-Phase Induction Motors on Unbalanced Voltages [Includes Discussion]," *Transactions of the American Institute of Electrical Engineers, Part III: Power Apparatus and Systems*, vol. 73, no. 2, pp. 125-133, 1954. [CrossRef] [Google Scholar] [Publisher Link]

[28] Ching-Yin Lee, "Effects of Unbalanced Voltage on the Operation Performance of a Three-Phase Induction Motor," *IEEE Transactions on Energy Conversion*, vol. 14, no. 2, pp. 202-208, 1999. [CrossRef] [Google Scholar] [Publisher Link]

[29] Miloje Kostic, *Effects of Voltage Quality on Induction Motor's Efficient Energy Usage*, Induction Motors - Modelling and Control, no. 5, pp. 127-156, 2012. [CrossRef] [Google Scholar] [Publisher Link]

[30] Ion Boldea, and Syed A. Nasar, *The Induction Machine Handbook*, 1st ed., CRC Press, 2001. [CrossRef] [Google Scholar] [Publisher Link]

[31] Pragasen Pillay, and Marubini Manyage, "Loss of Life in Induction Machines Operating with Unbalanced Supplies," *IEEE Transactions on Energy Conversion*, vol. 21, no. 4, pp. 813-822, 2006. [CrossRef] [Google Scholar] [Publisher Link]

[32] L. Malesani, L. Rossetto, and P. Tenti, "Active Filter for Reactive Power and Harmonics Compensation," *1986 17th Annual IEEE Power Electronics Specialists Conference*, Vancouver, Canada, pp. 321-330, 1986. [CrossRef] [Google Scholar] [Publisher Link]

[33] M. El-Habrouk, M. K. Darwish, and P. Mehta, "A Survey of Active Filters and Reactive Power Compensation Techniques," *2000 Eighth International Conference on Power Electronics and Variable Speed Drives (IEE Conf. Publ. No. 475)*, London, UK, pp. 7-12, 2000. [CrossRef] [Google Scholar] [Publisher Link]

[34] M. Takeda et al., "Harmonic Current and Reactive Power Compensation with an Active Filter," *19th Annual IEEE Power Electronics Specialists Conference*, Kyoto, Japan, pp. 1174-1179, 1988. [CrossRef] [Google Scholar] [Publisher Link]

[35] Hucheng Li et al., "Reactive Power Optimization of Distribution Network Including Photovoltaic Power and SVG Considering Harmonic Factors," *2017 International Conference on High Voltage Engineering and Power Systems (ICHVEPS)*, Bali, pp. 219-224, 2017. [CrossRef] [Google Scholar] [Publisher Link]

[36] Oladokun E. Faduyile, "*Effect of Harmonics on the Efficiency of a Three Phase Energy Efficient and Standard Motors*," Masters Theses, University of Tennessee at Chattanooga, 2009. [Google Scholar] [Publisher Link]

[37] G. Dinesh, "A Modified Self Tuning Fuzzy Logic Controller for Brushless Direct Current Motor," *International Journal of Recent Engineering Science*, vol. 1, no. 1, pp. 22-27, 2014. [Publisher Link]

[38] Tien-Dung Nguyen et al., "A New Optimizing Approach to Minimize Power Losses of an Electric Power Grid Containing Major Loads of Huge Power 3-Phase Induction Machines-A Practical Case Study in Vietnam," *SSRG International Journal of Electrical and Electronics Engineering*, vol. 10, no. 5, pp. 36-47, 2023. [CrossRef] [Google Scholar] [Publisher Link]

[39] EASA, Advice: Effects of High or Low Voltage on Motor Performance, EASA, The Electro-Mechanical Authority, 2000. [Online]. Available: https://easa.com/resources/resource-library/advice-effects-of-high-or-low-voltage-on-motor-performance

Appendix

Table 5. System parameters under study

Parameters	Value	Unit
$U_{ht1} = m.U_{dm}$		kV
U_{dm_DC}	400	V
R_{td}	0.0022	Ω
X_{td}	0.00892	Ω
P_{sum}	545	kW
Q_{sum}	337.8	kVAr
ΔU		kV
U_{TC}		kV
Δp_{bTrt}	$15*10^{-3}$	kW/ kVAr
K_1 (NEMA factor)	-1/58	n/a
K_2 (NEMA factor)	1.02/29	n/a
C (NEMA factor)	-1/55.75	n/a

Table 6. Parameters of IM 1 and cable 1

IM 1 and Cable 1	Value	Unit
R_1	0.053	Ω
X_1	0.009	Ω
P_1	160	kW
Q_1	99.16	kVAr
$\cos\varphi$	0.85	
Δp_b	$1*10^{-3}$	kW/kVAr

Table 7. Parameters of motor 2 and cable 2

IM 2 and Cable 2	Value	Unit
R_2	0.088	Ω
X_2	0.015	Ω
P_2	200	kW
Q_2	123.95	kVAr
$\cos\varphi$	0.85	
Δp_b	$1*10^{-3}$	kW/kVAr

Table 8. Parameters of motor 3 and cable 3

IM 3 and Cable 3	Value	Unit
R_3	0.070	Ω
X_3	0.012	Ω
P_3	185	kW
Q_3	114.65	kVAr
$\cos\varphi$	0.85	
Δp_b	$1*10^{-3}$	kW/kVAr